P.C. Lallana, C. Vázquez, B. Vinouze. ”Advanced multifunctional optical switch for multimode optical fiber networks”. In *Optics Communications*, 258 (2012) 12-June, pp. 2802-2808. Available in http://dx.doi.org/10.1016/j.optcom.2012.01.068

Advanced multifunctional optical switch for multimode optical fiber networks

P.C. Lallana [a,*], C. Vázquez [a,1], B. Vinouze [b,2]

[a] Electronics Technology Department, Carlos III University, C/ Butarque 15, 28911, Leganés, Madrid, Spain
[b] Optics Department, CNRS 6086 Foton Telecom Bretagne, Technopôle Brest-Iroise, CS 83818-29238 Brest Cedex 3, France

Abstract: In this work, an advanced multifunctional optical switch based on multimode fibers is proposed. It can work as a 3×1 optical multiplexer/combiner, a 2×2 optical switch, a variable optical attenuator and a variable optical power splitter. All these functionalities can be developed in the same device without any hardware modification, only by using the proper ports and control electronics.

The proposed switch has been developed for being used in the visible and near infrared wavelength range: 450–650 nm for optical fiber automobile applications, 650–850 nm for home broadband applications; and 850–1300 nm for multimode fiber access networks. Up to three different types of twisted nematic liquid crystal cells have been designed and fabricated for fulfilling these different wavelength ranges as part of the proposed device.

The multifunctional switch has been implemented and experimentally tested. Crosstalk usually better than −15 dB at 532 nm, 660 nm and 850 nm, in any state has been measured. Switching is achieved at voltage levels of 4 Vrms. Fiber to fiber insertion losses when operating as a 2×2 optical switch, range from 10 to 15 dB within 200 nm wavelength range; with a non-optimized optics for collimation and coupling.

Keywords: Liquid crystals, Optical switches, Optical multiplexer, Variable optical attenuators, Variable optical splitters, Fiber optics.

1. Introduction

Multimode fibers (both silica and polymer) with larger core diameters and numerical aperture, allow for large tolerance on axial misalignments, which results in cheaper connectors as well as associated equipment, but with a bandwidth penalty with regards to their singlemode counterparts, mainly due to the introduction of modal dispersion. On the other hand, polymer optical fiber (POF) offers several advantages over conventional multimode optical fiber over short distances (ranging from 100 m to 1000 m). POF is more flexible and ductile, making it easier to handle. Consequently, POF termination can be realized faster and cheaper than in the case of multimode silica fiber. Therefore, the number of applications that use POF is quickly increasing. POF is being used in video transmission in medical equipment, or in multimedia applications for civil aviation and high range cars [1], in-home [2] and access networks, wireless LAN backbone or office LAN and intrinsic optical sensor networks [3] among others.

In [4], two visible wavelengths (495 nm and 650 nm) are multiplexed on a 20 m POF link, allowing full duplex communication. Another coarse wavelength division multiplexing (WDM) over POF is shown in [5], in a simultaneous duplex data and a voice signal transmission. In automobile networks, different protocols are transmitted at specific wavelengths [6]. But greater channel capacity can be available using perfluorinated graded-index POF (PF GIPOF), with low attenuation and large bandwidth from 650 nm to 1300 nm [7]. Transmission of 10 Gbps data over 100 m and transmission of 1.25 Gbps Ethernet over 1 km have been experimentally demonstrated with PF-GIPOF [8]. On the other hand, combiners and multiplexers are basic elements in POF networks using WDM and there are not that many already developed. It is important to have low losses and reconfiguration can be an additional feature in those networks. Ideal passive combiners made up of cascading 2×2 directional couplers have high insertion losses, of at least 6 dB for a three input/one output port device. Reconfigurable optical networks in critical applications demand devices able to have different functionalities [9,10], including switching.

Many different switching technologies have been reported, and most of them could be applied to POF networks. Micro-electromechanical systems (MEMs) [11,12] that use mobile parts are attractive because of their large integration scale, good fiber-to-fiber coupling, high speed and crosstalk. An additional large optical fiber displacement 1×2 switch is presented in [13]. Switches based on liquid crystal cells are used because they do not have mobile parts, need low excitation voltages and have low power consumption. Two different kinds of liquid crystal are mostly used in switching technology: ferroelectric liquid crystals (FLC) [14,15] and nematic liquid crystals (NLC) [16–26]. First ones have better response times, but they can operate in a smaller wavelength

* Corresponding author. Tel.: +34 916248865; fax: +34 916249430.
E-mail addresses: pcontrer@ing.uc3m.es (P.C. Lallana), cvazquez@ing.uc3m.es (C. Vázquez), bruno.vinouze@telecom-bretagne.eu (B. Vinouze).
[1] Tel.: +34 916249191; fax: +34 916249430.
[2] Tel.: +33 229001526.

range because FLC cell thickness, d, should be different in order to obtain a polarization shift of 90° at each wavelength. Birefringence of this material, Δn, depends on the wavelength, λ, and the $\Delta n \times \lambda$ product must be constant to get the desired polarization switch. On the other hand, NLC only have to fulfill Mauguin's regime, $\Delta n \times d/\lambda >> 1$, in order to obtain the polarization shift, and this relation is kept in a wider wavelength range. The proposed structure for the advanced multifunctional optical switch (AMOS) uses NLC cells because they are able of working in a wider wavelength range.

Some of the structures reported for implementing optical switches are complex and have a great amount of components [15,16,18]. In [17] less components are used, but a fiber optic circulator is needed. A switch based on polarizing beam splitters is given in [18], but it only works at a single wavelength. In [19] a simple structure capable of working in a wider wavelength range is proposed, but the structure can handle only one polarization, so half of the input power is lost. In [20] a 4×4 strictly non-blocking optical switch that can also treat one polarization is presented. A simple structure for implementing a 3×1 multiplexer with NLC and polarizing beam splitters is given in [21].

A special case of NLC is a polymer dispersed liquid crystal (PDLC); different switching structures have been proposed in literature that use PDLC as the active element [22–24].

As already reported, the integration of different functionalities in the same device is useful for achieving cost and losses reductions. There have been several integrating proposals: a compact optical cross-connect add-drop switch based on NLC [25], a scalable holographic optical switch based on FLC [26], a smart value-added module, or tap coupler, that allows different tap ratios [27], or an integration of an optical switch with optical splitting and attenuating functions [9] with a non-liquid crystal technology. Most of the proposals given above operate in the 1550 nm wavelength range with a maximum bandwidth of 60 nm; they usually integrate just 2 functionalities and are not suitable for being used in broadband multimode fiber networks.

In the present work, an advanced multifunctional optical switch in a simple structure for being used in broadband POF networks is presented. Section two includes the description of the proposed structure, the design guidelines are given and the different functionalities are described. Section three comprises the experimental set-up and the measurements done for testing the device. Finally, some conclusions are given.

2. Device structure and operation principle

The structure for the advanced multifunctional optical switch (AMOS) is shown in Fig. 1 [28]. It is made of polarizing beam splitters (PBS), twisted nematic liquid crystal cells (TN-LC) and lenses. Three pairs of inputs are provided for multiplexing (if there are different wavelengths in each input) or combining. Any multimode fiber such as polymer optical fiber (POF) or graded-index POF (GI-POF) can be used as input and output ports.

AMOS is capable of treating both linear polarizations. The input PBS, "*PBS1*", splits the incoming light from each input port into two orthogonal independent linear polarized beams. P-Polarized light passes through the PBS, while S-Polarized light is reflected at 45°. Each of the obtained light beams is handled by one TN-LC cell. Both cells are controlled with the same square wave. Switching is obtained by applying voltage to the TN-LC cells. Two PBS, "*PBS2*" and "*PBS3*", are placed after each TN-LC cell for acting like analyzers. These two PBS are similar to "*PBS1*" and they work in the same way, S-Polarized light is reflected at 45°, and P-Polarized light is transmitted. Two lenses focus the beams in the output ports. Additionally, a lens is placed in each input port, in order to collimate the light from the input fiber.

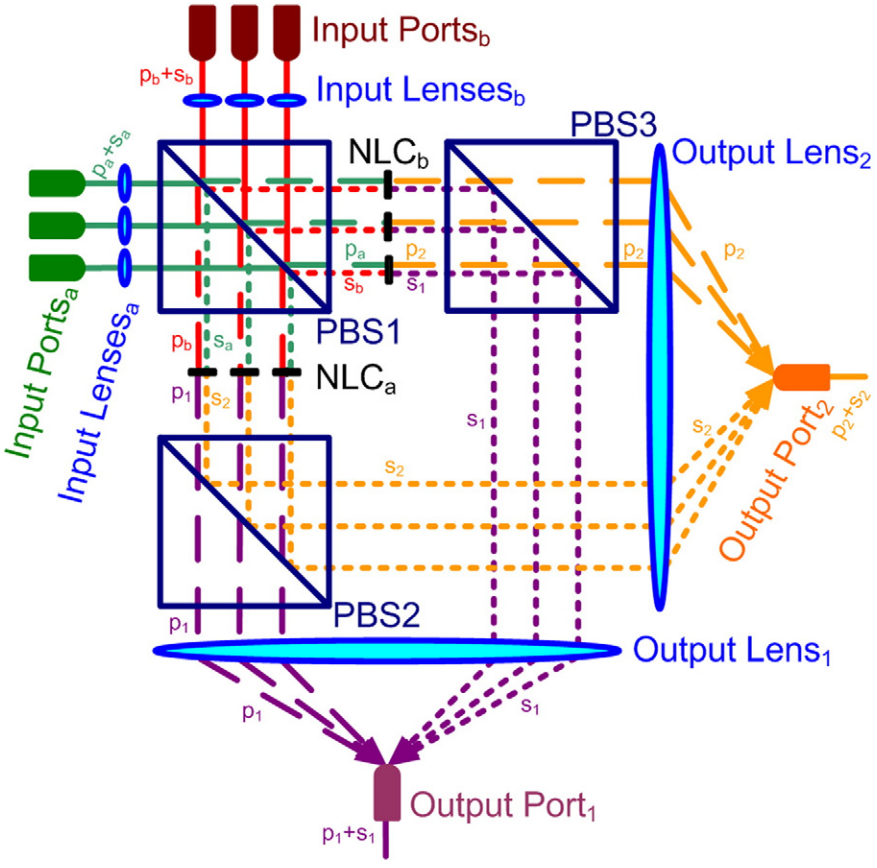

Fig. 1. Structure of the proposed advanced multifunction optical switch (AMOS).

The TN-LC cells modify their optical behavior depending on the applied voltage. The input light polarization is shifted when no voltage is applied to TN-LC cell, on the other hand, when an electric field is applied, LC molecules are reoriented, and the input light polarization remains the same when light passes through the cell. Thus, light path can be controlled by means of the TN-LC cells in combination with polarized filters.

One of the main characteristics of step index (SI) POF is its large core, 980 μm, and its high numerical aperture (NA), near 0.5. These two properties allow an easy light coupling into the output port of the device. Thanks to this, only by using a focusing lens, most of the guided power that arrives to the output port can be coupled to the output fiber. But there is a compromise between output focusing lenses parameters such as diameter (D) and focal length (f), and the optical fiber numerical aperture (NA) to allow the coupling of enough output power:

$$\mathrm{NA} > \arctan\left(\frac{\mathrm{D}}{2\cdot \mathrm{f}}\right) \tag{1}$$

It is also a scalable device, because more input channels can be added. The maximum number of channels is mainly limited by the size of the two output lenses and by the size of LC pixels. Output lens size, or diameter, is also dependent on the NA of output optical fibers as described above; and pixel size depends on the non-ideal collimated beam spot at each input. Each pixel of the TN-LC cell has to be larger enough for covering the beam spot of the input port. This beam spot depends on the input collimating lenses that define the beam size and the divergence of the non-ideal collimated beam.

2.1. Operation principle

The description of how the switching can be accomplished is detailed in the following.

In OFF state, when no voltage is applied to the TN-LC cell, the light beam from "*Input Port a*", IP3a, is guided to "*Output Port 1*", OP1, and consequently, the matched "*Input Port b*", $IP3_b$, is directed to "*Output Port 2*", OP2. Fig. 2 (a) shows the propagation when the device is in "*OFF*" state. Light beam from "*Input Port a*" is split by "*PBS1*" into two polarized beams, P-Polarized light is transmitted while S-Polarized light is reflected at 45°. On one hand, the polarized light that passes through "*PBS1*" is shift by the TN-LC cell named "*NLCb*" (see Fig. 1 for notation), and the resulting ray, which is S-Polarized, is reflected 45° by "*PBS3*" towards "*Output Lens 1*". On the other hand, the beam that is reflected 45° by "*PBS1*" is modified by "*NLCa*", the P-Polarized ray obtained passes through "*PBS2*" and is able to reach to "*Output Lens 1*". Finally, both beams are focused in "*Output Port 1*" by "*Output Lens 1*". Light can be coupled to the output fiber thanks to the high numerical aperture of POFs. In a similar way, "*Input Port b*" is guided to "*Output Port 2*".

In ON state, see Fig. 2 (b), when the TN-LC cells are switched through applied voltage, the "*Input Port a*", IP3a, is coupled to "*Output Port 2*", OP2, and the corresponding "*Input Port b*", $IP1_b$, is guided to "*Output Port 1*", PO1. Light from "*Input Port a*" is split by "*PBS1*"; P-Polarized light passes through it while the S-Polarized beam is reflected at 45°. In one optical path, beam passing through "*PBS1*" goes through "*NLCb*" and remains P-Polarized. The obtained ray passes also through "*PBS3*" and is able to reach to "*Output Lens 2*". On the other optical path, the S-Polarized beam is reflected by "*PBS1*", passing through "*NLCa*" and is reflected at 45° by "*PBS2*" towards "*Output Lens 2*". Finally, both beams are focused on "*Output Port 2*". In a similar way, "*Input Port b*" is directed to "*Output Port 1*", which is the opposite behavior of the OFF state.

Each pixel of the TN-LC cell can be switched independently of the others, so the proposed device can also works as a multiplexer, if there is a different wavelength in each input, or as a combiner. An optical path can be switched by applying voltage, or nor, on the suitable pair of pixels.

A summary of the ports used and the control signals are reported in Table 1 (See Fig. 1 and Fig. 2 for notation).

2.2. Functionalities

The proposed device can perform different functionalities without any hardware change, only by using the proper number of input and output ports and control electronics. It can be used as a 3×1 optical multiplexer/combiner (OM/OC), a 3×1 dual optical multiplexer/combiner (DOM/DOC), a 2×2 optical switch (OS), a variable optical attenuator (VOA) or a variable optical power splitter (VOPS).

If only one set of the inputs and one output are used, the device can operate like a 3×1 optical multiplexer/combiner, as shown in [21]. Device inputs are wavelength independent, so several wave-lengths can be combined into a single output optical fiber. Time divi-sion multiplexing (TDM) can also be implemented by means of this device, by allowing in a certain period of time the pass of one single input to the output. Moreover, even a mixture of a TDM and a WDM, i.e, different fibers involving WDM can be temporally com-bined into a single output fiber. Also a simple combination of the op-tical power at each input can also be developed.

When both sets of inputs and both outputs are used, the device operates as a dual 3×1 optical multiplexer (DOM), as shown in

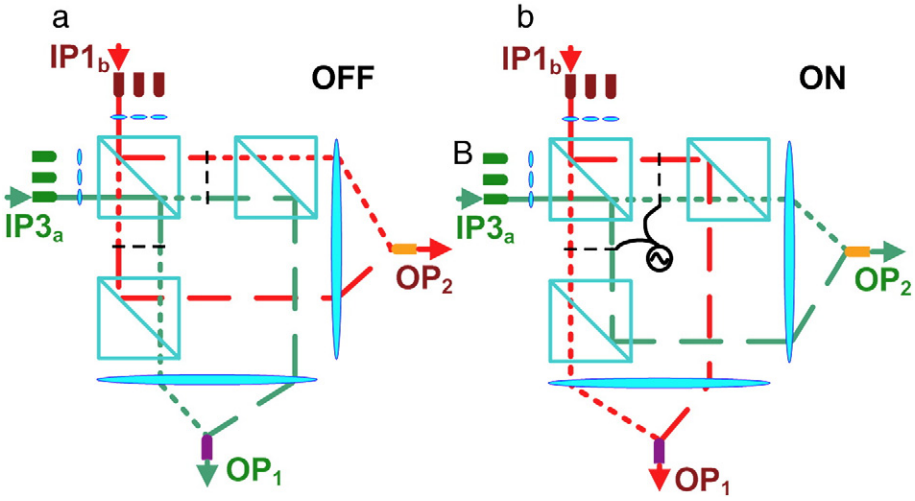

Fig. 2. OFF state (a) and ON state (b) of the proposed device (— P-polarization, - - - S-polarization).

Table 1
Summary of the ports used, the control signal and the TN-LC states for the Dual 3×1 multiplexer functionality.

Input ports	TN-LC states	Output port 1	Output port 2	Dual Mux state
IP1a & IP1b	Off	IP1a	IP1b	Off
	On	IP1b	IP1a	On
IP2a & IP2b	Off	IP2a	IP2b	Off
	On	IP2b	IP2a	On
IP3a & IP3b	Off	IP3a	IP3b	Off
	On	IP3b	IP3a	On

[28]. Inputs to the device are grouped in pairs, when the "*Input Port a*" is guided to "*Output Port 1*", the other input of this pair, "*Input Port b*", is coupled to "*Output Port 2*". On the other hand, when the corresponding channel of the multiplexer is switched, "*Input Port a*" is linked to "*Output Port 2*" and the matched "*Input Port b*" is propagated to "*Output Port 1*".

The proposed device can work as a 2×2 optical switch (OS) by using only one pair of inputs. An overview of this usage is shown in Fig. 2.

By using only one of the input and output ports of the AMOS, a VOA is developed when applying lower voltage to the NLC cells; for achieving intermediate transmission levels, see Fig. 3 (a).

Finally, in the same way, by applying different voltage levels to the liquid crystal cells, and using both outputs, as it is shown in Fig. 3 (b), AMOS can also operate as a VOPS, because the remaining light that is not guided to the desired output appears in the other output port.

3. Measurements and discussion

Specific TN-LC cells have been designed for allowing a broad wavelength range AMOS operation. In this sense, AMOS should be able to work in POF networks, such as, in automotive applications operating in the 450 nm–650 nm range, or in-home networks working at 650 nm. Even, the proposed device can also work in the 850–1300 nm wavelength range where GI-POF networks can operate.

According to the wavelength ranges shown above, three different types of TN-LC cells have been manufactured. The NLC used in the fabrication of the cells is a non-commercial mixture with very high birefringence (0.38 at 633 nm). Table 2 shows the main characteristics of the manufactured cells.

Table 2
Properties of the manufactured TN-LC cells.

	Wavelength range	Cell thickness
Cells no 1 & 7	400 nm–1300 nm	7 μm
Cells no 2 & 5	850 nm–1300 nm	11 μm
Cells no 3 & 8	400 nm–850 nm	15 μm

The structure of the manufactured cells is given in the Fig. 4 (a). Each cell has 3 pixels that allow the switching of three different pairs of input ports. The cells have been manufactured with usual TN-LC fabrication methods.

A photograph of the top view of the AMOS is shown in Fig. 4 (b). Three uncoated wire grid polarizing beam splitters PBS02A from Moxtek, two 11 μm thick nematic liquid crystal cells optimized for working in the 850 nm–1300 nm wavelength range (cells 2 & 5, see Table 2) and two 50 mm diameter plane-convex lenses with 75 mm focal length have been used. The use of uncoated PBS and NLC allow their operation in a wide wavelength range, although more reflections are expected. Experimental set up is shown in Fig. 5.

In the first set of measurements, two visible laser diodes have been used in the characterization. One laser diode at 650 nm and 5.0 mW from Power Technology Inc has been placed at the "*Input Port a*", and a laser diode at 532 nm and 1 mW from Hero has been placed at the "*Input Port b*". No input lenses have been employed because the laser diodes have in-built collimation optics.

SI POF has been used in both output ports. Each port has been measured independently of the others. A Hewlett Packard wave generator has been used for applying voltage to the liquid crystal cells. A 10 kHz frequency square wave with different voltage levels has been applied to the suitable pair of pixels in order to characterize the device transmission at both wavelengths.

In the second set of measurements, a multimode 62.5/125 μm fiber collimated by a GRIN lens has been used at the input port. Two 99:1 couplers have being used for measuring the switch fiber to fiber insertion losses and the switch crosstalk. As optical source, a dual LED from Ratioplast Optoelectronic with two interchangeable LEDs at different wavelengths (660 nm and 850 nm) has been utilized.

Two GRIN lenses have also been used for collimating the light beam at the output of the multimode fiber. A small stretch of fiber,

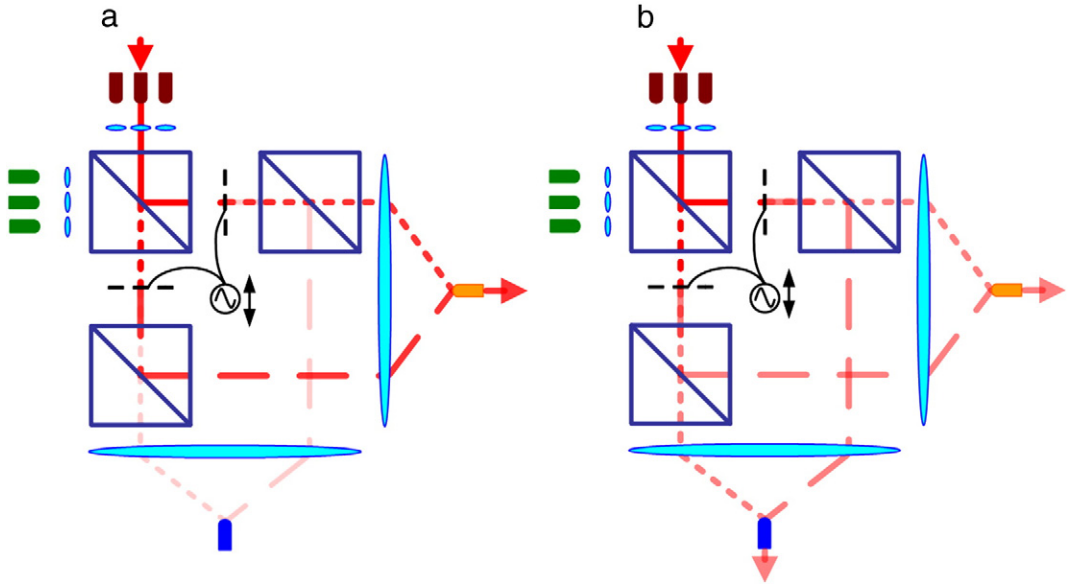

Fig. 3. Overview of the device operation as a VOA (a), and a VOPS (b) (<-> Voltage amplitude variation).

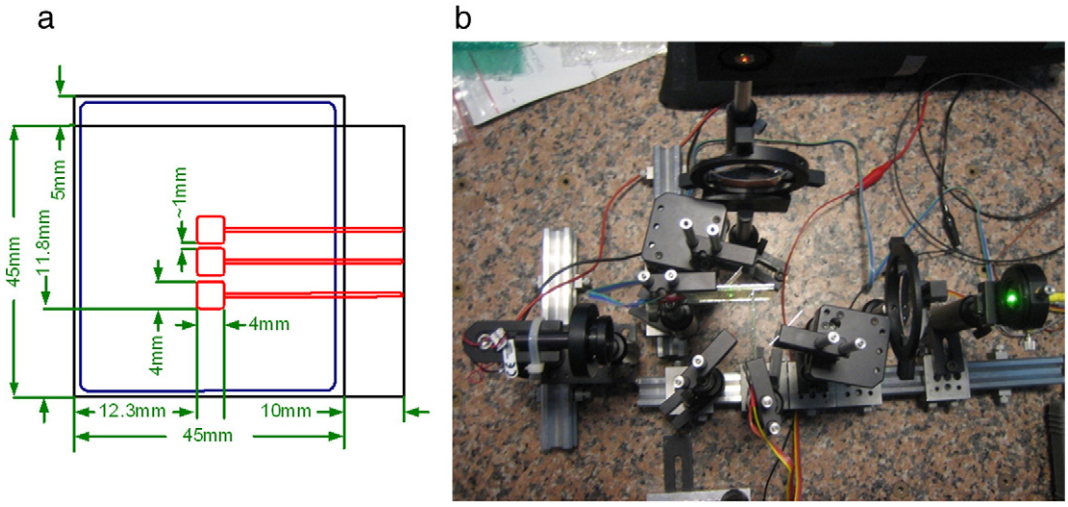

Fig. 4. Structure of the manufactured TN-LC cells (a) and a picture of the top view of the implemented device (b).

smaller than 20 cm has been used for guiding light from the output port to an amplified photodiode PDA100A from Thorlabs. Output voltages have been measured using a TDS1012 oscilloscope from Tektronix.

Measurements have been done using all the manufactured cell types and they have been characterized at two wavelengths, 660 nm and 850 nm.

The first measurements have been taken in two different steps for each pixel of the proposed device. In a first step, light from the laser diode at 650 nm was measured in both outputs. In the second step, light from the laser diode at 532 nm was also measured in both outputs. Fig. 6 shows the transmission measured for all the 3 pixels at both wavelengths. Measurements show a crosstalk, defined by Eq. (2), greater than −14 dB at both wavelengths and when a voltage of 4 Vrms is applied to any cell.

$$CT(dB) = 10 \cdot \log\left(\frac{P_{\text{no selected output}}}{P_{\text{in}}}\right) \quad (2)$$

As it was stated in section two, when no voltage is applied to the liquid crystal cells, "*Input Port a*" is guided to "*Output Port a*" and "*Input Port b*" is directed to "*Output Port b*". In the experimental set up used, when the laser diode at 650 nm ("*Input Port a*") is used, high optical power of light is measured in "*Output Port 1*" while low optical power is measured in "*Output Port 2*". The same happens with the light from the 532 nm laser diode.

The optical transmission of the device is modified when the voltage applied to both TN-LC cells is increased. Finally, when the cells are completely switched, the device is in ON state: light from "*Input Port a*" is guided to "*Output Port 2*" and light from "*Input Port b*" is directed to "*Output Port 1*". In the experimental set up used, there is more optical power from the 650 nm laser diode ("*Input Port a*") in "*Output Port 2*". And vice versa, more transmission from the 532 nm laser diode ("*Input Port b*") is measured in "*Output Port 1*".

The experimental results obtained in the second set of measurements are summarized in Table 3. Measurements show a crosstalk switch, defined by Eq. (2), greater than −13 dB at both wavelengths and in any status, and values of −24 dB are also achieved. Switching is achieved at voltage levels of 4 Vrms. Fiber to fiber insertion losses range from 10 to 15 dB within a 200 nm wavelength range. These high insertion losses, defined by Eq. (3), can be produced in part, by the divergence of the input beam that makes the output beam not

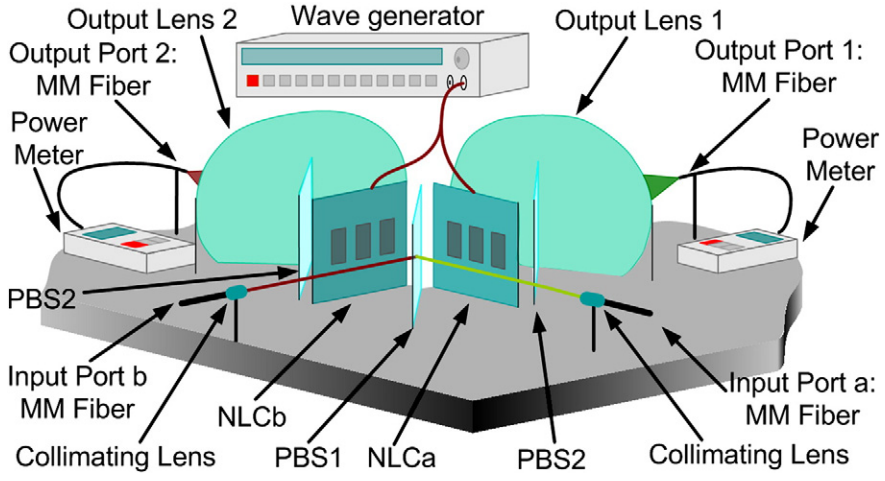

Fig. 5. Experimental set up.

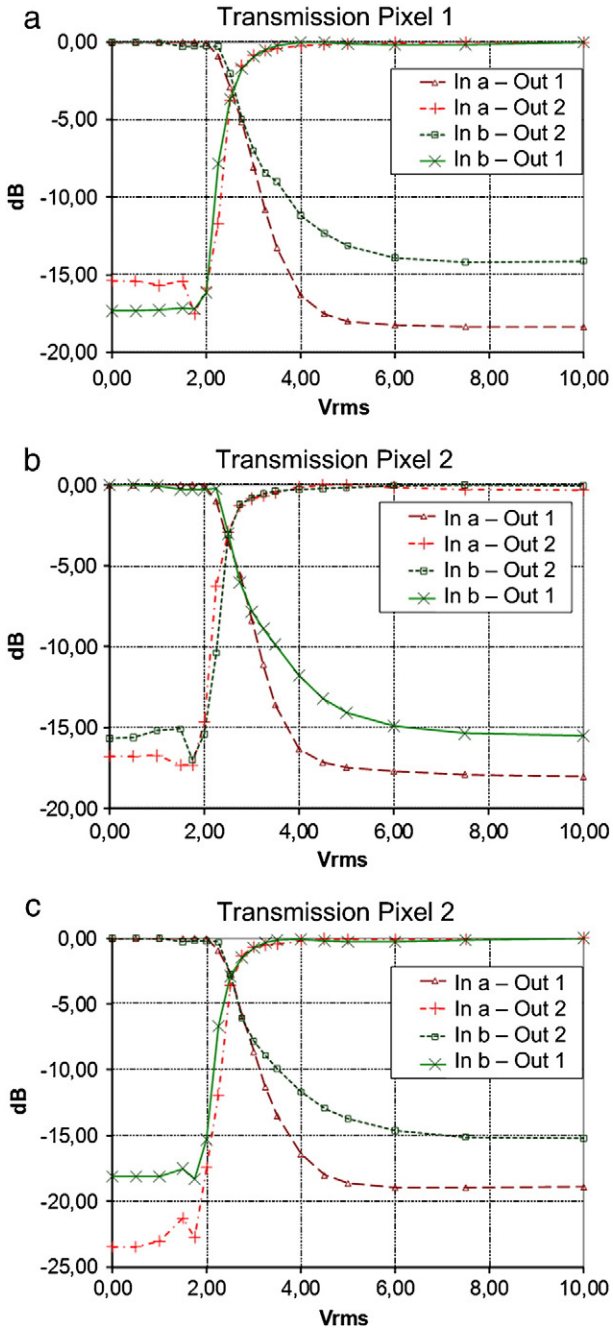

Fig. 6. Transmission measured versus the applied voltage at each pixel of the device.

to be well focused in the output fiber. This issue can be improved by using a fiber lens in the output port in order to collect more light. Insertion losses smaller than 5 dB can be estimated from the insertion losses measured at all individual bulk elements involved in building the AMOS.

$$IL(dB) = -10 \cdot \log\left(\frac{P_{selected\ output}}{P_{in}}\right) \quad (3)$$

The multiplexer proposed in [21] exhibits a crosstalk of -23 dB at 650 nm. It was implemented with conventional twisted nematic liquid crystal cells and cube PBSs that have higher extinction ratios. In the present work, the use of uncoated wire grid polarizers instead of cube PBSs make possible the use of the device in a wide wavelength range but smaller extinction ratios and higher insertion losses have been obtained.

AMOS operation as a VOA and a VOPS has also been test. Fig. 7 shows AMOS transmission in both outputs, "*Output Port 1*" and "*Output Port 2*", when "*Input Port b*" is excited. In VOPS both outputs ports "1" and "2", have to be considered, while only one should be taken into account under VOA operation. From Fig. 7, it is shown that both functionalities can be achieved approximately from 2 Vrms to 3 Vrms. As an example, a 50:50 splitting ratio is obtained for 2.5 Vrms, but different coupling ratios could be achieved by adjusting the voltage applied to the TN-LC cells.

Finally, in order to make a dynamic characterization of the AMOS operating as an optical switch, three laser modules at different wavelength: 532 nm, 650 nm and 850 nm have been placed at "*Input Port b*" instead of the multimode fiber and the GRIN lenses, and the optical power has been measured in both output ports. Measurements have been done with all the manufactured cells. A 5 Vrms amplitude and 10 kHz square wave has been applied to the TN-LC cells during 0.5 s and 0 V has been applied for other 0.5 s. Thus, the measured response times of the AMOS as an optical switch are summarized in Table 4.

Greater response times of the LC correspond with its relaxation time. According to the device implementation, the rise time when the optical power is measured in "*Output Port 1*" corresponds with the excitation time of the LC, while the fall time is related with the LC relaxation time. On contrast, the relaxation time of LC matches up with the rise time when the output light is measured in "*Output Port 2*". For this reason, different response times are obtained for the AMOS depending on the selected output.

Moreover, thinner LC cells exhibit shorter response times than wider ones. Thus, response times when cells 3 & 8 are used are three times the response times when cells 1 & 7 are utilized. In addition, greater response times of the AMOS than those shown by the isolated LC cells are also expected. It can also be observed that there is not a high dependence with the wavelength; response times are in the same order of magnitude. Fig. 8 shows the rise times for the three wavelengths used in the characterization when cells 2 & 5 are used in the implementation of the AMOS.

Because of multimode fiber high NA, collimated light beam can have more divergence. In our set-up, an average 4° beam divergence is estimated, which will be reduced in the future for improving losses. As stated above, our AMOS is a scalable device. In order to obtain an estimation of the maximum number of input channels, a pixel size of 9 mm has been considered with SI POF, and a 4 mm pixel with GI-POF. Under these assumptions, and using a 50 mm diameter output lens, the maximum number of channels should be of 6 for POF networks and of 18 for GI-POF applications.

4. Conclusions

Broadband advance multifunctional optical switches (AMOS) for networks using multimode fibers have been proposed. 3×1 optical

Table 3
Characterization of the AMOS as an optical switch when different TN-LC cells are used.

Cells no 1 & 7 (400 nm–1300 nm)		Insertion losses (dB) (fiber–fiber)		Crosstalk (dB)	
Input	Output	660 nm	850 nm	660 nm	850 nm
Ports a	Port 1	13.12	11.98	−15.88	−18.77
Ports a	Port 2	14.21	12.25	−14.20	−18.24
Ports b	Port 1	15.15	11.25	−17.62	−14.80
Ports b	Port 2	15.55	10.93	−15.96	−13.60
Cells no 2 & 5 (850 nm–1300 nm)		Insertion losses (fiber–fiber)		Crosstalk	
Ports a	Port 1	12.84	11.90	−23.70	−18.38
Ports a	Port 2	13.51	11.91	−18.38	−18.51
Ports b	Port 1	13.20	11.06	−23.70	−16.14
Ports b	Port 2	15.33	10.81	−14.88	−16.14

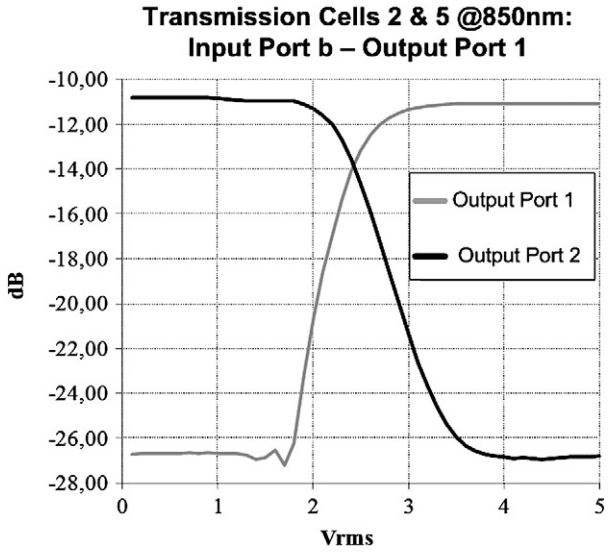

Fig. 7. Transmission measured versus the applied voltage from Input Port B to Output Port 1 and Output Port 2 when Cells 2 & 5 are used in the AMOS.

multiplexer/combiner, dual 3×1 optical multiplexer/combiner, 2×2 optical switch (OS), variable optical attenuator (VOA) and variable optical power splitter (VOPS) can be implemented in the same device by selecting the proper ports (through control electronics) without any hardware modification.

Thanks to the use of twisted nematic liquid crystal (TN-LC) cells, low voltage square wave is required for switching and low power consumption is expected. TN-LC cells operating in a broad wavelength range: 530 nm, 650 nm, 850 nm and 1300 nm are fabricated. The proposed structure is scalable, in the present design up to 6 input ports could be implemented in POF applications, and up to 18 input ports for GI-POF or standard silica multimode fiber applications.

The proposed structure has been implemented and experimentally tested. Crosstalks usually better than −15 dB at 532 nm, 660 nm and 850 nm, in any state have been reported. Switching is achieved at voltage levels of 4 Vrms. Fiber to fiber insertion losses in AMOS operating as a 2×2 OS, range from 10 to 15 dB within a 200 nm wavelength range; with a non-optimized optics for collimation and coupling. Switching times depends on the TN-LC cells thickness, and varies from tens to hundreds of milliseconds in the implemented AMOS.

Broadband VOA and VOPS can be obtained by applying intermediate voltage levels to the TN-LC cells, ranging from 2 to 6 Vrms.

Finally, the proposed scheme can be used in multimode optical networks as a reconfigurable device. It can be used in broadband networks, in the visible and near infrared wavelength range: 450–650 nm for automobile applications, at 650–850 nm for home broadband applications; and with graded index POF working in the 850–1300 nm wavelength range for coarse wavelength division multiplexing (CWDM) broadband access and sensor networks.

Table 4
Response times of the AMOS as an optical switch when different TN-LC cells are used.

Input port b	Rise time (ms)			Fall time (ms)		
Cells 1 & 7	532 nm	650 nm	850 nm	532 nm	650 nm	850 nm
Output Port 1	10.10	8.60	8.40	33.20	39.80	42.40
Output Port 2	38.80	39.40	40.00	20.50	24.30	17.28
Cells 2 & 5						
Output Port 1	24.40	21.00	14.40	73.93	73.80	94.80
Output Port 2	70.60	76.30	101.60	59.80	23.00	15.20

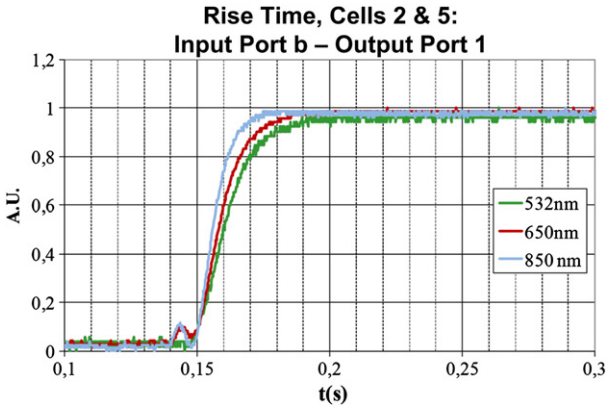

Fig. 8. Rise times from Input Port b to Output Port a of the AMOS implemented with cells 2 & 5 at different wavelengths. A 10 Vrms square wave is applied when low transmission is obtained.

Acknowledgements

This work was partially supported by CICYT (TEC2009-14718-C03-03-MCI), by the European Commission through the NoE BONE (Project no. 216863), and FACTOTEM-II-CM: S2009/ESP-1781 Projects. Thanks to J. M. S. Pena, D. S. Montero and J. M. Otón for the comments.

References

[1] T. Kibler, S. Poerl, G. Böck, H.P. Huber, E. Zeeb, Journal of Light Technology 22 (9) (2004) 2184.
[2] http://gigaset.com/hq/en/product/GIGASETOPTICALLANADAPTERDUO.html 2010. Available on 25th of May.
[3] C. Vázquez, A.B. Gonzalo, S. Vargas, J. Montalvo, Sensors and Actuators A116 (2004) 22.
[4] M. Yonemura, A. Kawasaki, S. Kato, M. Kagami, Y. Inui, Optics Letters 30 (17) (2005) 2206.
[5] Y. Zhang, H. Ma, T. Zhang, Z. Wang, D. Wang, R. Zheng, H. Yang, H. Ming, Proceedings of SPIE 5644 (2005) 835.
[6] M. Kagami, R&D Review of Toyota 40 (2) (2005).
[7] J. Goudeau, G. Widawski, B. Bareel, 13th International Plastic Optical Fibers Conf, 76, 2004.
[8] S.C.J. Lee, F. Breyer, S. Randel, B. Spinnler, I.L. Lobato Polo, D. Van Den Borne, J. Zeng, E. De Man, H.P.A. Van Den Boom, A.M.J. Koonen, Optical Fiber Communication and the National Fiber Optic Engineers Conference 2007 OFC/NFOEC 2007, 2007.
[9] Q.H. Chen, W.G. Wu, Z.Q. Wang, G.Z. Yan, Y.L. Hao, Optics Communication 281 (2008) 5049.
[10] C. Vázquez, P.C. Lallana, D.S. Montero, J. Montalvo, VI symposium on Enabling Optical Nerworks (SEON 2008), Porto (Portugal), 2008.
[11] C. Marxer, N.F. De Rooij, Journal of Light Technology 17 (1) (1999) 2.
[12] R.A. Jensen, LEOS´02 I (2002) 230.
[13] M.I. Bhuiyan, Y. Haga, M. Esashi, Journal of Quantum Electronics 41 (2) (2005) 242.
[14] N.A. Riza, S. Yuan, Journal of Light Technology Letters 17 (1999) 1575.
[15] N.A. Riza, S. Yuan, Electronics Letters 5 (1998) 1341.
[16] R.A. Soref, Optics Letters 6 (6) (1981) 275.
[17] S. Sumriddetchkajorn, N.A. Riza, D. Sengupta, Optical Engineering 40 (2001) 1521.
[18] N.A. Riza, Optics Letters 19 (1994) 1780.
[19] C. Vázquez, J.M.S. Pena, A.L. Aranda, Optics Communication 224 (2003) 57.
[20] F. Pain, R. Coquillé, B. Vinouze, N. Wolffer, P. Gravey, Optics Communication 139 (1997) 199.
[21] P.C. Lallana, C. Vázquez, J.M.S. Pena, R. Vergaz, Opto-electronics Review 14 (4) (2006) 311.
[22] P.C. Lallana, C. Vázquez, B. Vinouze, K. Heggarty, D.S. Montero, Molecular Crystals and Liquid 502 (2008) 130.
[23] N.A. Riza, M. Madamopoulus, Optical Engineering 37 (11) (1998) 3061.
[24] N. Madamopoulus, N.A. Riza, Optics Communication 157 (1998) 225.
[25] J.S. Patel, Y. Silberberg, IEEE Photonics Technology Letters 7 (5) (1995) 514.
[26] W.A. Crossland, I.G. Manolis, M.M. Redmond, K.L. Tan, T.D. Wilkinson, M.J. Holmes, T.R. Parker, H.H. Chu, J. Croucher, V.A. Handerek, S.T. Warr, B. Robertson, I.G. Bonas, G. Frankling, C. Satace, H.J. White, R.A. Woolley, G. Henshall, Journal of Light Technology 18 (12) (2000) 1845.
[27] N.A. Riza, S.A. Reza, Applied Optics 46 (18) (2007) 3800.
[28] P.C. Lallana, C. Vázquez, D.S. Montero, K. Heggarty, B. Vinouze, 16th International Plastic Optical Fibers Conf, 2007, p. 63.